


Polarization and Weak Topology in Chern Insulators

Sachin Vaidya^{1,2,*}, Mikael C. Rechtsman,¹ and Wladimir A. Benalcazar^{3,†}

¹*Department of Physics, The Pennsylvania State University, University Park, Pennsylvania 16802, USA*

²*Department of Physics, Massachusetts Institute of Technology, Cambridge, Massachusetts 02139, USA*

³*Department of Physics, Emory University, Atlanta, Georgia 30322, USA*

 (Received 25 April 2023; revised 8 November 2023; accepted 30 January 2024; published 15 March 2024)

Chern insulators, and more broadly, topological insulators, present an obstruction to the construction of exponentially localized electronic Wannier functions. This implies a fundamental difficulty in determining whether such insulators exhibit electric polarization. Here, we show that these insulators can indeed exhibit bound charges and adiabatic currents consistent with changes in bulk polarization over space and time, respectively. We also show that the change in polarization across crystalline domains within these strong topological insulators is quantized in the presence of crystalline symmetries.

DOI: [10.1103/PhysRevLett.132.116602](https://doi.org/10.1103/PhysRevLett.132.116602)

The concept of electric polarization is essential for understanding insulating materials and topological phases of matter. Although heuristically understood as the electric dipole moment per unit volume, its determination in crystalline materials is subtle [1,2]. In the 1990s, a correct definition of polarization was formulated in terms of the Berry phase of the Bloch wave functions across the Brillouin zone [1–6]. The Berry phase encodes the positions of the spatially resolved Wannier functions, so-called “Wannier centers,” which further facilitates establishing the bulk-boundary correspondence for polarization. However, recent explorations of topological insulators have revealed that a Wannier representation is not always possible [7,8] and thus, whether the concept of polarization can be extended beyond the Wannier center picture has gained relevance and remains an open question in topological band theory.

In this Letter, we show that Chern insulators can exhibit electric polarization. Our argument circumvents the seemingly ill-defined nature of the bulk polarization in these insulators by observing that the physical manifestations of polarization—electronic bound charges and adiabatic currents—are proportional to *changes in polarization*, and not the polarization itself. We demonstrate that these changes are well defined in Chern insulator phases. Furthermore, we show that under crystalline symmetries, the bound charges that appear at interfaces between crystalline domains within these insulators are fractionally quantized, carrying topological states along with them. Finally, we develop a finer topological identification and classification that captures the physical observables at these crystalline domain interfaces. We construct our arguments using two systems: a tight-binding model and an experimentally realizable microwave photonic crystal, both with nonvanishing Chern number, and then generalize our observations to the case of time-reversal polarization in quantum spin Hall (QSH)

insulators and 3D topological insulators (TI). Our work settles a long-standing question and deems bulk polarization as the fundamental quantity with a “bulk-boundary correspondence,” regardless of whether a Wannier representation is possible.

In crystalline insulators, the electric polarization \mathbf{P} is defined in terms of Berry phases along the noncontractible loops of the Brillouin zone [4] or, equivalently, in terms of the Wannier centers of the occupied bands [1,9,10]. In 2D crystalline insulators with primitive lattice vectors $\mathbf{a}_{i=1,2}$, the bulk polarization $\mathbf{P} = P_1 \mathbf{a}_1 + P_2 \mathbf{a}_2$ has components $P_i = \oint d^2 \mathbf{k} \text{Tr}[\mathcal{A}_i(\mathbf{k})]$, where \mathcal{A}_i is the Berry connection with components $[\mathcal{A}_i(\mathbf{k})]_{m,n} = -i \langle u_m(\mathbf{k}) | \partial_{k_i} | u_n(\mathbf{k}) \rangle$, and $|u_m(\mathbf{k})\rangle$ is the Bloch eigenstate of occupied band m at crystal momentum $\mathbf{k} = (k_1, k_2)$. The components of \mathbf{P} can also be written as $P_i = \oint dk_j p_i(k_j)$, where

$$p_i(k_j) = \frac{1}{2\pi} \oint dk_i \text{Tr}[\mathcal{A}_i(\mathbf{k})] \pmod{1} \quad (1)$$

is the k_j sector polarization, for $i, j = 1, 2; i \neq j$.

Chern insulators are paradigmatic topological materials that are insulating in the bulk but have conducting chiral edge states [7,8]. In Chern insulators, $p_i(k_j)$ winds around the 1D Brillouin zone formed by $k_j \in [-\pi/a_j, \pi/a_j]$. This winding simultaneously reflects the difficulty in building exponentially localized Wannier functions [11,12] and defining the bulk polarization [13]. Furthermore, the chiral edge states that cross the Fermi level complicate establishing the bulk-boundary correspondence to polarization because the bound charge, if it exists, would be affected by the partial occupation of its chiral edge states [13].

To address the question of polarization in strong topological insulators, our starting point is to focus on the

associated physical observables. Consider the interface between two insulating domains, R_1 and R_2 . A charge density σ arises due to the *difference in polarization* across this interface, following the ‘‘interface-charge theorem’’ [1,5],

$$\sigma = [\mathbf{P}^{(R_1)} - \mathbf{P}^{(R_2)}] \cdot \hat{\mathbf{n}} \pmod{1}, \quad (2)$$

where we have set the unit cell lengths in all directions and the electronic charge to unity for simplicity, and $\hat{\mathbf{n}}$ is the vector normal to the interface. If domains R_1 and R_2 have unequal Chern numbers, i.e., $C_1 \neq C_2$, $|C_1 - C_2|$ topologically protected chiral edge states will appear at their common interface, rendering it metallic. This, in conjunction with the aforementioned winding of $p_i(k_j)$, makes the definition of polarization and its bulk-boundary correspondence problematic. Coh and Vanderbilt studied how a definition of the polarization might be saved in the case $C_1 = 1$, $C_2 = 0$, but only with the knowledge of the wave vector at which the (partial) occupancy of the edge state is discontinuous [13].

Here, we instead consider Chern insulator domains in which $C_1 = C_2$, such that $p_i^{(\alpha)}(k_j)$ [Eq. (1)], for domains $\alpha = \{R_1, R_2\}$, individually wind, but where the difference in k -sector polarizations across the two domains, $\Delta p_i(k_j) = p_i^{(R_1)}(k_j) - p_i^{(R_2)}(k_j)$, does not wind, and is nonzero. The key insight here is that this configuration preserves the non-trivial nature of the Chern insulator but allows for insulating interfaces between crystalline domains within its bulk, which can be probed for responses to spatial changes in polarization. As we shall see, this insight will enable a physical notion of polarization that yields measurable observables, i.e., bound charges consistent with Eq. (2). We will also show that adiabatic variations of polarization within Chern insulators can result in the pumping of charges via currents. Taken together, both observables (bound charges and currents) are sufficient to demonstrate that crystals without a Wannier representation can exhibit a response to polarization.

We first present the accumulation of electronic bound charge at the interface between crystalline domains within a Chern insulator using a two-band tight-binding model described by the following generalized Qi-Wu-Zhang (QWZ) Hamiltonian,

$$h_{\text{QWZ}}(\mathbf{k}, \theta) = \sin k_x \sigma_x + \sin(k_y + \theta) \sigma_y + [m + \cos k_x + \cos(k_y + \theta)] \sigma_z. \quad (3)$$

Here $\mathbf{k} = (k_x, k_y)$ is the crystal momentum, $\sigma_{x,y,z}$ are the Pauli matrices and m is a mass term. For $\theta = \theta^* = 0$ and π , this Hamiltonian possesses inversion symmetry, $\mathcal{I}h(\mathbf{k}, \theta^*)\mathcal{I}^{-1} = h(-\mathbf{k}, \theta^*)$, with $\mathcal{I} = \sigma_z$. The Hamiltonian in (3) is gapped for all values of \mathbf{k} and θ . The value of m sets the Chern number C for the bands, with $C = 1$ for

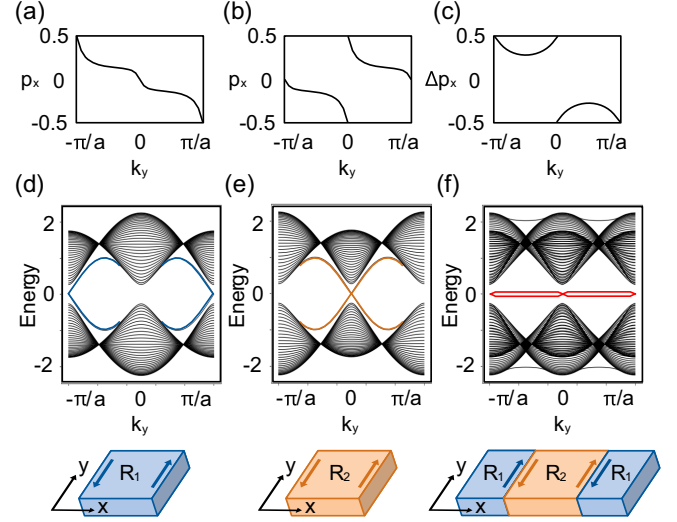


FIG. 1. (a),(b) $p_x(k_y)$ for the occupied band of $h_{\text{QWZ}}(\mathbf{k}, 0)$ and $h_{\text{QWZ}}(\mathbf{k}, \pi)$, respectively, for $m = 0.25$. (c) $\Delta p_x(k_y)$ for $h_{\text{QWZ}}(\mathbf{k}, 0)$ and $h_{\text{QWZ}}(\mathbf{k}, \pi)$. (d),(e) Energy bands for $h_{\text{QWZ}}(\mathbf{k}, 0)$ and $h_{\text{QWZ}}(\mathbf{k}, \pi)$, respectively, with open boundaries as depicted in the bottom panels. The chiral edge states are highlighted in blue and orange. (f) Energy bands for an inversion-symmetric configuration consisting of two domains described by $h_{\text{QWZ}}(\mathbf{k}, 0)$ and $h_{\text{QWZ}}(\mathbf{k}, \pi)$ as depicted in the bottom panel. The system has periodic boundaries imposed along both directions and has two internal interfaces. The nonchiral edge states at these interfaces are highlighted in red.

$0 < m < 2$. The plots of $p_x(k_y)$ for $m = 0.25$ and for $\theta^* = 0$ and π exhibit a nontrivial winding due to a nonzero Chern number [Figs. 1(a) and 1(b)]. Under open boundaries along one direction, i.e., with vacuum on the exterior, these systems host chiral edge states as seen from their energy bands [Figs. 1(d) and 1(e)].

We now consider two adjacent domains, R_1 and R_2 , with Bloch Hamiltonians $h_{R_1}(\mathbf{k}) = h_{\text{QWZ}}(\mathbf{k}, 0)$ and $h_{R_2}(\mathbf{k}) = h_{\text{QWZ}}(\mathbf{k}, \pi)$, respectively. Although h_{R_1} and h_{R_2} have a winding in $p_i(k_j)$, the quantity $p_i^{(1)}(k_j) - p_i^{(2)}(k_j)$ does not wind [Fig. 1(c)] [14]. Crucially, the difference in polarization across the interface separating the two domains, ΔP_i , given by

$$\Delta P_i = \oint dk_j \Delta p_i(k_j), \quad (4)$$

is quantized to $\frac{1}{2}$, due to inversion symmetry.

To explore the consequences of this non-zero difference in polarization, we consider a finite, inversion-symmetric system that consists of the two domains described by h_{R_1} and h_{R_2} as shown at the bottom of Fig. 1(f). In this system, we observe the appearance of nonchiral edge states in the energy bands [Fig. 1(f)]. As a result of this and the presence of inversion symmetry, fractional charge densities (per unit length) quantized to $\pm \frac{1}{2}$ appear at each of the two interfaces

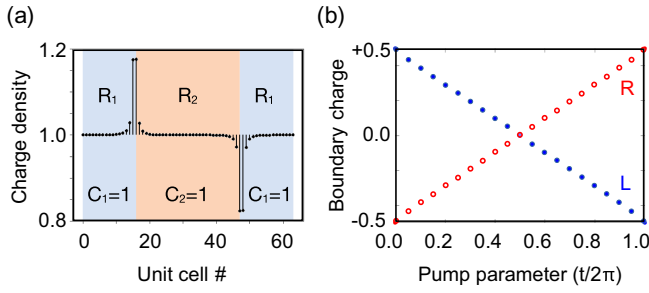


FIG. 2. (a) The charge density at half filling for the system shown in Fig. 1(f). Under inversion symmetry, the bound charges at the interfaces are quantized to ± 0.5 . (b) The bound charges at the left (L) and right (R) interfaces under an adiabatic change in the polarization as a function of t . Inversion symmetry is present at $t/2\pi = 0$ and 0.5 .

at exactly half filling [15] [Fig. 2(a)]. This is consistent with the theorem in Eq. (2) and is analogous to the expected response to polarization in conventional insulators. We emphasize that the distinction between the two Chern insulator domains is solely due to crystalline symmetry. Breaking this symmetry can render them indistinguishable without closing the band gap.

We next turn our attention to the second physical observable associated with polarization—a current density in the bulk that appears due to an adiabatic change in polarization in time. We probe the existence of bulk currents via the bound charges that appear at crystalline domain interfaces within a Chern insulator in the system considered above. To show this, we adiabatically evolve the domain R_2 in Fig. 1(f), by changing the parameter θ as $\theta(t) = t + \pi$, i.e., $h_{R_2} = h_{\text{QWZ}}(\mathbf{k}, t + \pi)$ for the parameter $t \in [0, 2\pi)$, while keeping the domain R_1 constant, i.e., $h_{R_1} = h_{\text{QWZ}}(\mathbf{k}, 0)$. The two domains remain gapped in the bulk for the full cycle of the adiabatic parameter. During a single pump cycle, we observe that the bound charges exhibit a change of ± 1 unit of charge [Fig. 2(b)]. The fact that a single unit of charge is pumped during the cycle at the boundaries implies, by continuity, that this charge is also pumped from the left to the right of each unit cell, giving rise to a current density in the bulk of the Chern insulator domain R_2 . While this last statement would be trivial in the case of a Wannierizable system, it is not so in the absence of a Wannier representation.

We have seen that inversion symmetry quantizes the difference in polarization in Chern insulators to 0 or $\frac{1}{2}$, and, correspondingly, the bound charges to 0 or $\pm \frac{1}{2}$ units. This implies the existence of *weak* topological phenomena [16] at crystalline interfaces within inversion-symmetric Chern insulators. To explore this further, we consider the description of inversion-symmetric insulators using symmetry indicators.

A set of crystalline energy bands in class A of the tenfold classification under inversion symmetry is characterized by an index given by [17–20]

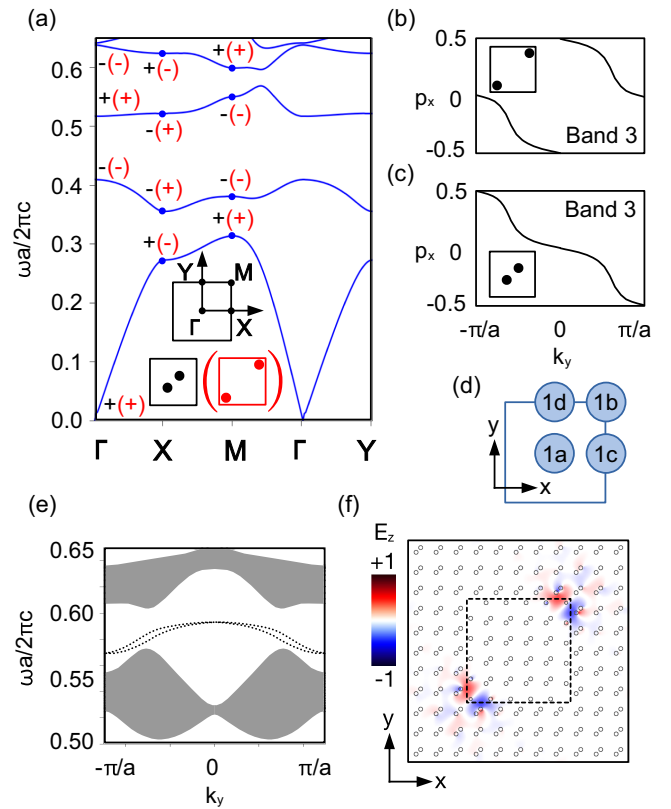


FIG. 3. (a) The transverse magnetic (TM) band structure of the photonic crystals with unit cells shown in the inset. The high-symmetry points are labeled by inversion eigenvalues for both unit cell configurations. (b),(c) The Wilson loop spectrum of band 3 for the contracted and expanded unit cells, respectively. (d) Maximal Wyckoff positions in an inversion-symmetric unit cell. (e) The frequency spectrum of an inversion-symmetric system made of the two types of unit cells with two interfaces. In-gap edge states (dotted lines) are localized at the interface between the two domains. (f) The E_z mode profile for corner states that arise at the corners between the two Chern photonic crystals in a “core-cladding” geometry. The inner core domain (dashed box) consists of the expanded unit cell type and the outer cladding domain consists of the contracted unit cell type.

$$\chi = \left(C | [X], [Y], [M] \right), \quad (5)$$

where C is the Chern number and the symmetry indicators $[\Pi]$ are defined as $[\Pi] \equiv \#\Pi - \#\Gamma$, where $\#\Pi$ is the number of states within the bands of interest with inversion eigenvalue $+1$, at the high-symmetry point (HSP) Π . The set of single isolated Wannierizable bands can be enumerated exhaustively starting from symmetric Wannier functions centered at maximal Wyckoff positions [Fig. 3(d)] [21–23] (see Ref. [24] for more details).

Insulators with a vanishing Chern number, whose occupied bands are characterized by the index χ are deformable to either *atomic limits* or *fragile* phases. For such insulators, the polarization (with respect to vacuum)

can be calculated as $\mathbf{P}(\chi) = (1/2)([Y] + [M])\mathbf{a}_1 + (1/2)([X] + [M])\mathbf{a}_2$, where \mathbf{a}_1 and \mathbf{a}_2 are the primitive lattice vectors [17,18]. Additionally, some configurations can lead to higher-order topological corner states for both atomic limits and fragile phases, determined by the corner charge index $Q(\chi) = (1/4)(-[X] - [Y] + [M])$ [17,18,25]. Both $\mathbf{P}(\chi)$ and $Q(\chi)$ are defined modulo a unit electronic charge.

For a pair of Chern insulator domains characterized by indices χ_1, χ_2 , with the same Chern number $C_1 = C_2 = C$, the relative index, $\Delta\chi = \chi_2 - \chi_1$, defined as $\Delta\chi = (C_2 - C_1|[X]_2 - [X]_1, [Y]_2 - [Y]_1, [M]_2 - [M]_1)$, has a vanishing Chern component and describes either an atomic limit or a fragile phase. As a result, while $\mathbf{P}(\chi_\alpha)$ and $Q(\chi_\alpha)$ for $\alpha \in \{1, 2\}$, are ill defined for the Chern insulators individually, the difference in polarization, $\Delta\mathbf{P} := \mathbf{P}(\Delta\chi)$, and relative corner charge index, $\Delta Q := Q(\Delta\chi)$, are meaningful. These quantities are associated with physical observables, i.e., edge and corner states are expected to appear at the interface between the Chern insulator domains described by χ_1 and χ_2 , with nonzero $\Delta\mathbf{P}$ and ΔQ .

In the tight-binding example studied in Fig. 1(f), we have already seen the appearance of such edge states induced by a nonzero difference in polarization across the boundary. We now show the generality of this framework by demonstrating the presence of polarization-induced edge and corner states in experimentally realizable microwave photonic crystals (PhCs) that do not admit a tight-binding description [26–30].

The unit cells of the proposed inversion-symmetric, two-dimensional PhCs consist of two dielectric discs made out of yttrium-iron-garnet (YIG) ($\epsilon = 15$), a strong magneto-optical material at microwave frequencies [inset Fig. 3(a)]. These two unit cell types are related by a shift of $a/2$ in both x and y directions, where a is the lattice constant, and we refer to them as “contracted” and “expanded.” Time-reversal symmetry is broken by applying a magnetic field in the z direction. We calculate the band structure for PhCs with these unit cells using the *MIT Photonic Bands* package [31] [Fig. 3(a)]. Using the inversion eigenvalues at HSPs for both unit cell types, we determine the χ indices and $\Delta\chi$ for the first four TM bands (see Ref. [24] for details). This analysis shows that bands 1 and 2 are atomic limits, with Wannier centers at the $1a$ ($1b$) position for the contracted (expanded) unit cell. Band 3 acquires a Chern number of $+1$ for both unit cell types [Figs. 3(b) and 3(c)], and similarly, band 4 has a Chern number of $+1$. For all four bands, the difference in polarization between the contracted and expanded PhCs, $\Delta\mathbf{P}$, is equal to $\frac{1}{2}(\mathbf{a}_1 + \mathbf{a}_2)$, and the relative corner charge index, ΔQ , is equal to $\frac{1}{2}$.

To explore the bulk-boundary correspondence associated with nonzero $\Delta\mathbf{P}$ and ΔQ for the Chern bands, we first simulate a configuration consisting of an inner domain with the expanded unit cell and an outer domain consisting of the contracted unit cell, as shown in Fig. 1(f). We observe

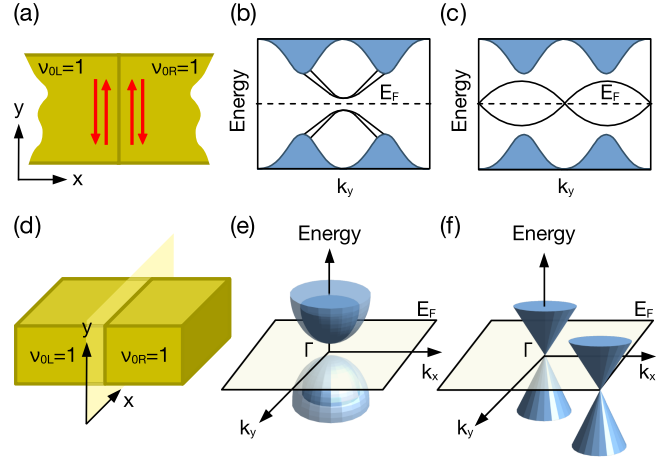


FIG. 4. (a) An interface between two quantum spin Hall insulators with the same nontrivial \mathbb{Z}_2 invariant can host either (b) a gapped trivial phase where the two pairs of helical edge states cross at the same TRIM point and hybridize or (c) a gapless nontrivial phase where the two pairs of helical edge states cross at different TRIM points. (d) An interface between two 3D TIs with the same strong invariant can host either (e) a gapped trivial phase where the two surface Dirac cones sit at the same TRIM point and hybridize or (f) a gapless nontrivial phase where the two surface Dirac cones sit at different TRIM points. E_F marks the Fermi level.

that the frequency spectrum contains polarization-induced nonchiral edge states, similar to those found in the tight-binding example [Fig. 3(e)]. We note that such edge states have been previously reported in PhC- and waveguide-based systems and may be useful for certain photonic applications [32,33]. Next, we simulate a finite system in a “core-cladding” type of geometry and find corner states [Fig. 3(f)]. Using a filling anomaly argument, we show in [24] that the edge and corner states originate from multiple Chern bands and, therefore, have a topological origin [17,18]. The observed boundary states thus clearly demonstrate the meaningfulness of $\Delta\mathbf{P}$ and ΔQ as weak topological invariants in Chern insulators.

The weak topological phenomenon discussed so far can be extended to QSH and 3D TI cases. In Fig. 4(a), we consider the interface between two crystalline domains in a QSH insulator with a nontrivial \mathbb{Z}_2 invariant, $\nu_0 = 1$. Its boundary with vacuum hosts helical edge states that are Kramers degenerate at time-reversal invariant momentum (TRIM) points [34,35]. However, the interface between the two QSH domains, at half filling, can either exhibit trivial gapped states, when the helical edge states of each domain cross and hybridize at the same TRIM point [Fig. 4(b)], or (weak) topological gapless states, where the helical edge states of each domain cross at different TRIM points [Fig. 4(c)]. Although the two QSH domains have the same nontrivial strong \mathbb{Z}_2 invariant, the presence or absence of boundary states at their common interface is characterized by the difference in time-reversal polarization, which is a

weak \mathbb{Z}_2 invariant [36]. A similar argument applies to 3D TIs protected by a strong topological index ν_0 [37] [Figs. 4(d)–4(f)].

In this Letter, we have argued that strong topological insulators (Chern insulators, QSH insulators, 3D TIs) can exhibit a well-defined response to electric polarization because they manifest its associated bulk-boundary correspondence and transport properties. To unveil this, we have used interfaces across different crystalline domains within the same strong topological phase as probes, thus avoiding the gapless boundary modes originating from strong topology. The presence of crystalline symmetries quantizes the responses, making the polarization a weak topological index that determines the existence of first- and higher-order topological states, which can be explored in various platforms such as the proposed photonic crystals [30], optical waveguide arrays [33,38,39], coupled ring resonators [40], as well as in topological insulators with grain boundaries [41].

We note that previous works have found other manifestations of bound charge and responses to weak indices in Chern insulators, such as at dislocations and disclinations [42–47].

We acknowledge fruitful discussions with Jeffrey Teo, Thomas Christensen, Ali Ghorashi, and Marius Jürgensen. M. C. R. and S. V. acknowledge the support of the U.S. Office of Naval Research (ONR) Multidisciplinary University Research Initiative (MURI) under Grant No. N00014-20-1-2325 and the Charles E. Kaufman Foundation under Grant No. KA2020-114794. W. A. B. acknowledges the support of startup funds from Emory University.

*svaidya1@mit.edu

†benalcazar@emory.edu

- [1] D. Vanderbilt, *Berry Phases in Electronic Structure Theory: Electric Polarization, Orbital Magnetization and Topological Insulators* (Cambridge University Press, Cambridge, England, 2018).
- [2] R. Resta and D. Vanderbilt, *Theory of Polarization: A Modern Approach. In: Physics of Ferroelectrics. Topics in Applied Physics* (Springer, Berlin, Heidelberg, 2007).
- [3] J. Zak, *Phys. Rev. Lett.* **62**, 2747 (1989).
- [4] R. Resta, *Rev. Mod. Phys.* **66**, 899 (1994).
- [5] D. Vanderbilt and R. D. King-Smith, *Phys. Rev. B* **48**, 4442 (1993).
- [6] R. D. King-Smith and D. Vanderbilt, *Phys. Rev. B* **47**, 1651 (1993).
- [7] X.-L. Qi, Y.-S. Wu, and S.-C. Zhang, *Phys. Rev. B* **74**, 085308 (2006).
- [8] F. D. M. Haldane, *Phys. Rev. Lett.* **61**, 2015 (1988).
- [9] N. Marzari, A. A. Mostofi, J. R. Yates, I. Souza, and D. Vanderbilt, *Rev. Mod. Phys.* **84**, 1419 (2012).
- [10] C. Brouder, G. Panati, M. Calandra, C. Mourougane, and N. Marzari, *Phys. Rev. Lett.* **98**, 046402 (2007).
- [11] T. Thonhauser and D. Vanderbilt, *Phys. Rev. B* **74**, 235111 (2006).
- [12] D. Thouless, *J. Phys. C* **17**, L325 (1984).
- [13] S. Coh and D. Vanderbilt, *Phys. Rev. Lett.* **102**, 107603 (2009).
- [14] It is assumed here that the two bulk materials share the same periodicity and that the same choice of gauge is made for their Berry connections, \mathcal{A}_1 and \mathcal{A}_2 , in Eq. (1).
- [15] An infinitesimal breaking of inversion symmetry is necessary to lift the degeneracy of edge states, only one of which is occupied at half filling. This breaking of inversion symmetry fixes the sign of the fractional charges at each boundary.
- [16] “Weak” topological phenomena here refers to those protected and enforced by crystalline symmetries (as opposed to the strong topological phenomena of the tenfold classification).
- [17] W. A. Benalcazar, T. Li, and T. L. Hughes, *Phys. Rev. B* **99**, 245151 (2019).
- [18] S. Vaidya, A. Ghorashi, T. Christensen, M. C. Rechtsman, and W. A. Benalcazar, *Phys. Rev. B* **108**, 085116 (2023).
- [19] A. Alexandradinata, X. Dai, and B. A. Bernevig, *Phys. Rev. B* **89**, 155114 (2014).
- [20] T. L. Hughes, E. Prodan, and B. A. Bernevig, *Phys. Rev. B* **83**, 245132 (2011).
- [21] B. Bradlyn, L. Elcoro, J. Cano, M. Vergniory, Z. Wang, C. Felser, M. I. Aroyo, and B. A. Bernevig, *Nature (London)* **547**, 298 (2017).
- [22] J. Cano, B. Bradlyn, Z. Wang, L. Elcoro, M. G. Vergniory, C. Felser, M. I. Aroyo, and B. Andrei Bernevig, *Phys. Rev. B* **97**, 035139 (2018).
- [23] H. C. Po, A. Vishwanath, and H. Watanabe, *Nat. Commun.* **8**, 50 (2017).
- [24] See Supplemental Material at <http://link.aps.org/supplemental/10.1103/PhysRevLett.132.116602> for a discussion on indices for inversion-symmetric systems and a detailed analysis of the photonic crystal example.
- [25] Defining \mathbf{P} and \mathbf{Q} for fragile phases is a little more subtle. Fragile phases (F) have non-Wannierizable bands that can be formally expressed as differences of atomic limits (say A_1 and A_2) as $F = A_1 \ominus A_2$. Adding the correct atomic-limit degrees of freedom (in this case, A_2) to F renders the full set of bands Wannierizable. \mathbf{P} and \mathbf{Q} can be calculated for F by first calculating them for the Wannierizable set, $F \oplus A_2 = A_1$, and then removing the contribution from A_2 .
- [26] J. D. Joannopoulos, S. G. Johnson, J. N. Winn, and R. D. Meade, *Photonic Crystals: Molding the Flow of Light*, 2nd ed. (Princeton University Press, Princeton, NJ, 2008).
- [27] S. Raghu and F. D. M. Haldane, *Phys. Rev. A* **78**, 033834 (2008).
- [28] F. D. M. Haldane and S. Raghu, *Phys. Rev. Lett.* **100**, 013904 (2008).
- [29] Z. Wang, Y. D. Chong, J. D. Joannopoulos, and M. Soljačić, *Phys. Rev. Lett.* **100**, 013905 (2008).
- [30] Z. Wang, Y. Chong, J. D. Joannopoulos, and M. Soljačić, *Nature (London)* **461**, 772 (2009).
- [31] S. G. Johnson and J. D. Joannopoulos, *Opt. Express* **8**, 173 (2001).
- [32] J. Chen, W. Liang, and Z.-Y. Li, *Phys. Rev. B* **99**, 014103 (2019).
- [33] F. S. Piccioli, M. Kremer, M. Ehrhardt, L. J. Maczewsky, N. Schmitt, M. Heinrich, I. Carusotto, and A. Szameit, [arXiv:2202.03252](https://arxiv.org/abs/2202.03252).

- [34] B. A. Bernevig and S.-C. Zhang, *Phys. Rev. Lett.* **96**, 106802 (2006).
- [35] C. L. Kane and E. J. Mele, *Phys. Rev. Lett.* **95**, 146802 (2005).
- [36] L. Fu and C. L. Kane, *Phys. Rev. B* **74**, 195312 (2006).
- [37] L. Fu, C. L. Kane, and E. J. Mele, *Phys. Rev. Lett.* **98**, 106803 (2007).
- [38] M. C. Rechtsman, J. M. Zeuner, Y. Plotnik, Y. Lumer, D. Podolsky, F. Dreisow, S. Nolte, M. Segev, and A. Szameit, *Nature (London)* **496**, 196 (2013).
- [39] J. Schulz, S. Vaidya, and C. Jörg, *APL Photonics* **6**, 080901 (2021).
- [40] M. Hafezi, S. Mittal, J. Fan, A. Migdall, and J. Taylor, *Nat. Photonics* **7**, 1001 (2013).
- [41] H. W. Kim, S.-H. Kang, H.-J. Kim, K. Chae, S. Cho, W. Ko, S. Jeon, S. H. Kang, H. Yang, S. W. Kim *et al.*, *Nano Lett.* **20**, 5837 (2020).
- [42] W. A. Benalcazar, J. C. Y. Teo, and T. L. Hughes, *Phys. Rev. B* **89**, 224503 (2014).
- [43] T. Li, P. Zhu, W. A. Benalcazar, and T. L. Hughes, *Phys. Rev. B* **101**, 115115 (2020).
- [44] Y. Zhang, N. Manjunath, G. Nambiar, and M. Barkeshli, *Phys. Rev. Lett.* **129**, 275301 (2022).
- [45] Y. Zhang, N. Manjunath, G. Nambiar, and M. Barkeshli, *Phys. Rev. X* **13**, 031005 (2023).
- [46] F. Schindler, S. S. Tsirkin, T. Neupert, B. Andrei Bernevig, and B. J. Wieder, *Nat. Commun.* **13**, 5791 (2022).
- [47] H. Yoshida, T. Zhang, and S. Murakami, *Phys. Rev. B* **108**, 075160 (2023).